

# INVESTIGATION OF NEUTRONIC AND THERMAL-HYDRAULIC PERFORMANCE FOR HTR-10 UNDER NORMAL OPERATING CONDITIONS

S. KÖSE, İ. KILIÇ

Technology Department, Turkish Atomic Energy Authority, 06530, Ankara, Turkey

---

## ABSTRACT

The VSOP'94 code, obtained from OECD/NEA Data Bank, has been used for the neutronic and thermal-hydraulic prediction calculations for the initial core loading of the HTR-10 reactor. In the neutronic aspect of this study, double heterogeneity for the fuel element, buckling feedback in the spectrum calculation, and mixture of graphite and fuel balls are taken into account. The results, compared to a relevant study based on the first criticality experiment of HTR-10 [4], indicate that relative errors for the multiplication factor are less than 1.34%, being in a reasonable range.

In the thermal-hydraulic analysis, the power distribution obtained from the neutronic calculations is used where temperature and flow distributions are calculated for the reactor core. During the calculations, conservative hydraulics and physics parameters, such as minimum mass flow rates in the core, no radiation heat transfer in the axial direction, are used. The calculated maximum fuel centerline temperature is 927.4°C for normal operating conditions and observed not to exceed the safety limit [6].

## ÖZET

OECD Veri Bankasından temin edilen VSOP'94 bilgisayar programı kullanılarak HTR-10 reaktörünün ilk kor yüklemesine ait nötronik ve ısı-akışkan hesaplamaları gerçekleştirilmiştir. Çalışmanın nötronik kısmında, yakıt elemanları için çift heterojenlik, spektrum hesaplamalarında aki-

büküm geri beslemesi, grafit ve yakıt toplarının homojen karışımı göz önüne alınmıştır. Nötronik hesaplamalar, HTR-10'nun ilk kritiklik hesaplama sonuçlarını içeren başka bir çalışma ["Xingqing Jing, et al., Nuc. Eng. & Design-218, ,2002"] ile karşılaştırılmıştır. Analizin sonucunda, çoğalma faktöründeki görelî hataların, makul sınırlarda (maksimum %1.34'den düşük) olduğu gözlenmiştir.

Isıl-akışkan hesaplamalarda, nötronik hesaplamalarda elde edilen güç dağılım profilleri kullanılmıştır. Bu analizde basınç kabı içerisindeki sıcaklık ve akışkan dağılımları hesaplanmıştır. Hesaplamalarda, kordan minimum akış oranının geçirilmesi, eksensel yönde radyasyonel ısı aktarımının olmaması vb. gibi tutucu kabuller yapılmıştır. Normal işletme koşulları için, maksimum yakıt merkez sıcaklığı 927.4°C olarak hesaplanmıştır. Bu değerin normal işletme ve kaza koşulları için belirlenen sınır olan 1230 °C'nin altında kaldığı görülmüştür.

## 1. INTRODUCTION

International interest in the High Temperature Gas Cooled Reactor (HTGR) technology has been increasing in recent years due to their robust designs arising from highly inherent safety features, cost effective electricity generation that can be appropriate for the developing countries such as Turkey, as well as for providing high temperature process heat. The HTR-10, 10 MW High Temperature Gas Cooled pebble bed reactor is a remarkable prototype that has been recently connected to the grid at the beginning of 2003 in China.

The main goal of this study is to predict the steady state core physical behavior of HTR-10 initial core, calculated by using the VSOP [1] code package. The scope of these calculations includes determination of neutronic parameters such as effective multiplication factor ( $k_{eff}$ ) and core power peaking factors and thermal-hydraulic behavior during normal operating conditions.

## 2. METHODOLOGY

### 2.1 Neutronic Analysis

#### 2.1.1 Core Physics

The main physical parameters used in the calculations are given in Table 1 [2]. The reactor core cross sectional view is given in Figure 1. The core is of the pebble bed design in which fuel, in the form of “pebbles” that pass continuously through the core during normal operating conditions. Based on initial core loading, the fuel and graphite balls have a ratio of 0.57 and 0.43, respectively. There are total of 27000 balls in the full core.

#### 2.1.2 Code and method of calculations

In the neutronic analysis, VSOP computer code, which is suitable for the physical calculations and analysis of pebble bed high temperature gas-cooled reactor is used. The code uses two definite libraries, i.e. GAM and THERMOS, containing fast-epithermal and thermal cross-section data, respectively. In the GAM library there are 68 fine group cross-sections merged into 3 groups (10 MeV-52.5 KeV, 52.5 KeV-29 eV, 29-2.05 eV). In the resonance integral calculations,  $^{238}\text{U}$  resonances with an energy interval 4-4307 eV is considered. The THERMOS library contains 30 energy groups covering 0-2.05 eV range. In the spectrum calculations the thermal groups are merged into 1 energy group and neutronic analysis are performed over totally 4 energy groups.

In the fuel design, the code considers the graphite balls as dummy layers located at the outside of the fuel balls, as if it has a radius of 3.61823 cm, where radius of a fuel ball is 3 cm regarding fuel/graphite balls volume ratios. Hence, the envisaged fuel design in the calculations from inner region to outer region consists of fuel matrix containing homogenized coated particles, graphite shell and graphite moderator layer referring graphite dummy balls. Fuel design data used in the calculations are given in Table 2.

The geometric design of the reactor core is modeled in the two-dimensional r-z geometry. The diffusion code CITATION, incorporated in VSOP, serving as the neutronic solver is used for reactor calculations via the 4-group energy structure. The fuel elements containing the graphite layers

are homogeneously distributed in the core. The core is divided into batches representing different spectrum zones having different temperatures. The radial core channels are shown in Figure 2.

During the neutronic calculations, the following assumptions are taken into account:

- Double heterogeneity of the fuel elements
- Boron impurities in fuel elements and reflectors
- Buckling feedback in the spectrum calculations
- Anisotropic diffusion constant for the top cavity

There are 10 control rod channels, 7 elliptic boron absorber ball channels and 20 helium flow channels in the side reflector. Channels for control rods, boron absorber balls and helium flow are smeared in the side reflector located at the outer side of the core in r-z geometry, regarding conservation of volumes and distances from center of the core.

### 2.1.3 Results

The International Atomic Energy Agency (IAEA) has organized a physics benchmark of the HTR-10 initial core as part of its Coordinated Research Program [3]. Later, another study [4] has been performed for the calculations of  $k_{\text{eff}}$  for the initial core loading of HTR-10 for various loaded core heights and temperatures. This study has been also compared with experimental results and it shows predicted code calculations overlap with experimental results. Therefore, prior to neutronic calculations for full core, calculations of the effective multiplication factors are based on the same core configurations and temperatures. The results are given in Table-3 and Table-4 for 27°C and 50°C, respectively. Critical core heights are 118.27 cm for 27°C and 119.51 cm 50°C by using interpolation between  $k_{\text{eff}}$  values. Also, reactivity worth of control rods is calculated for 27°C. The effective multiplication factor for full core ( $h=197$  cm active core height) is predicted as 1.1645. In the case of fully inserted control rods  $k_{\text{eff}}$  is calculated to be 0.99048. So, total reactivity worth of the control rods is 149.43 mk ( $\Delta k/k$ ) at 27°C.

In the full core modeling, temperatures obtained from thermal-hydraulic calculations (by THERMIX) are used in order to obtain neutronic parameters. The corresponding spectrum zones based on these temperatures are used in diffusion core calculations. The effective multiplication factors with the definite spectrum zones are 1.1076 for start-up and 1.1013 for Xe-Sm

equilibrium core. Power peaking factors (*ppf*) for start-up core and equilibrium core are given in Figure 3 and Figure 4, respectively. Maximum *ppf*=1.292 occurs at R=0 cm in radial and Z=112.5 cm in axial direction from center and top of the equilibrium core. The power density corresponding to the maximum *ppf* at 10 MW is 2.585 MW/m<sup>3</sup>

## 2.2 Thermal-Hydraulic Analysis

### 2.2.1 Core parameters

Table 5 shows the basic thermal hydraulic parameters of the reactor. The core thermal output is nominally 10 MW. In the initial core loading, the graphite balls are uniformly distributed within the fuel balls due to reactivity reasons. The ceramic core structure consists of side, bottom and top reflectors, comprising 15 layers of graphite and carbon blocks along the core height (Figure 1). There are 20 gas boreholes in the side reflector for the coolant channels. The bottom reflector contains the hot gas plenum. There are ten reactor control and shutdown rod holes in the same side reflector. Seven small absorber ball shutdown units are designed for the second shutdown system when any control rods failure happens. The metallic components in the reactor consist of core barrel, bottom supporting structure and the top thermal shield, which support the whole reactor core and reflectors. During the reactor operation, the annular area between the reactor pressure vessel and the core barrel is filled with cold helium of 250°C to ensure the temperature of pressure vessel not to exceed the safety limits.

### 2.2.2 Thermal Hydraulic calculation

The calculations are performed with THERMIX/KONVEK code which was linked into the VSOP. The code calculates the temperatures and flow parameters for steady-state condition and transients. It performs the calculations in accordance with the relevant KTA-Standards [5] in German safety guide while solving the equations which represent the conservation laws; mass, momentum and energy.

In the initial flow distribution, the total inlet mass flow rate into the pressure vessel is 4.3 kg/s, of which 1% of the rated flow (0.043 kg/s) passes through the fuel discharge tube to cool the discharged fuel elements from the core, 2.5% (0.108 kg/s) of the rated flow passes through control rod

holes, 10% of the rated flow (0.43 kg/s) leaks into the graphite components and rest of the coolant, which corresponds to 86% of the rated flow (3.72 kg/s) passes through the reactor core to remove the heat generated by the fuel elements [6]. The gas flow model is shown in Figure 5 where there are 17 different flow regions divided into 17 radial and 25 axial mesh points. This model consists of the reactor core channels representing the pebble bed, plenums at the top and bottom of the pressure vessel, fuel discharge channel, control rod channel and leak flow channel in the side reflector. The channels, except the plenums, are considered to have a pipe flow characteristics. It is assumed that there is no flow resistance in the plenums.

The small flow channels embedded inside the bottom reflector of the core have two different flow areas, where the center section is larger than the outer section in order to reduce temperature difference at the core outlet. This effect is considered in the hydraulic modeling of flow channels at the bottom reflector (zone 5 and 15 given in Figure 5). For the helium leaks from the graphite components, a small pipe (zone 13) at the side reflector is modeled where there is no convective heat transfer through this pipe. Zone 12 is the leak path for the control rod holes.

In the thermal modeling, the tabulated formulas existing in the code are used for the thermal properties such as thermal conductivity, heat capacity of the materials (pebbles, reflector, brick, thermal shield, etc.).

Because of 0.57/0.43 fuel/moderator ball ratio, the heating factor of a single fuel ball is selected 1.76 instead of 1.0 .Power distribution obtained from neutronic analysis is used in the calculations.

### 2.2.3 Results

The heat removed by the coolant per unit volume in the core is shown Figure 6. 99.7% of the rated power generated in the core is removed by convective heat transfer mechanism. Rest of the rated power (0.3%) is transferred to the helium leaking through the reflector, the control rod holes and the helium flow channels passing outside of the core.

Helium, fuel surface and fuel centerline temperature distributions are shown in Figure 7, Figure 8 and Figure 9, respectively. The maximum fuel surface temperature is 865.9°C and the maximum fuel centerline temperature is 927.4°C (R=0 cm in radial and Z=210.4 cm in axial) that is lower than the maximum fuel temperature limit, 1230°C, under normal and accidental conditions based on the specifications [6]. Helium, fuel surface

and fuel centerline temperatures at  $R=0$  with respect to the axial direction are shown Figure 10. The helium temperature increases about  $6^{\circ}\text{C}$  through the flow channels before entering the core. The predicted outlet helium temperature at the bottom plenum is  $699.5^{\circ}\text{C}$ . The calculated pressure drop in the core is 1.28 kPa.

### 3. CONCLUSION

The results, when compared to the previous study for HTR-10 design [4] concerning  $k_{\text{eff}}$ , yields acceptable relative errors in the neutronic calculations, which are less than 1.34%. These errors arise from different nodalization of bottom conus of core, as well as from the usage of different energy widths for the generation of few group constants. The difference between the volumes of the actual geometry and the volumes modeled in the VSOP for the conus leads to error in mass for U-235 content in the core.

In the thermal-hydraulic calculations, results are consistent with the design specifications of HTR-10. Comparing the results with the study [6], concerning temperature distributions and flow characteristics, there are small differences ( $\leq 7^{\circ}\text{C}$ ) at the fuel and helium temperatures. The differences between these two studies could arise from the selection of different heating factor of a single fuel ball and using different power profiles obtained from the neutronic analysis. The results of the thermal-hydraulic analysis show that the safety requirements, such as maximum fuel temperature limit are satisfied.

### REFERENCES

- [1]. Teuchert E., Haas K.A., et al., 1994, VSOP-Computer code system for Reactor Physics and Fuel cycle Simulation. JÜLICH.
- [2]. Wolf L., Scherer W., et al., 1990, High temperature reactor core physics and reactor dynamics. Nucl. Eng. Des. 121, 227-240.
- [3]. IAEA-CRP, 2000, Evaluation of High Temperature Gas Cooled reactor performance- Physics benchmark results.
- [4]. Xingqing J., Xiaolin X., et al., 2002, Prediction calculations and experiments for the first criticality of the 10 MW High Temperature Gas Cooled Reactor-Test Module. Nucl. Eng. Des. 218, 43-49.

- [5]. KTA Standards, 3102.1 (1978), 3102.2 (1983), 3102.3 (1981), 3102.4 (1984), 3102.5 (1986)
- [6]. Zuying Gao, Lei Shi, 2002, Thermal hydraulic calculation of the HTR-10 for the initial and equilibrium core. Nucl. Eng. Des. 218, 51-64.

## TABLES AND FIGURES

**Table 1** Main design data for the HTR-10 core

**Table 2** Main design data for fuel and graphite ball for the HTR-10

**Table 3**  $k_{\text{eff}}$  versus core height for 27 °C

**Table 4**  $k_{\text{eff}}$  versus core height for 50 °C

**Table 5** HTR-10 Main Physical Parameters

**Figure 1** View of HTR-10 reactor

**Figure 2** Radial core channels modeled in VSOP

**Figure 3** Power peaking Factors for start-up core

**Figure 4** Power peaking Factors for Xe-Sm equilibrium core

**Figure 5** Hydraulic modeling of HTR-10 for the VSOP code

**Figure 6** Heat removal per unit volume from the core by helium flow

**Figure 7** Helium temperature distribution in the core

**Figure 8** Solid surface temperature distribution in the HTR-10

**Figure 9** Fuel centerline temperature distribution in the core

**Figure 10** Helium, fuel surface and fuel centerline temperatures at R=0 cm along the core axial direction



**Table 1.**

Physical Parameter	Value
Core equivalent diameter (cm)	180
Core equivalent height (cm)	196.5
Height of the top cavity (cm)	42
Thickness of the top reflector (cm)	90
Height of the bottom cone reflector (cm)	38
Thickness of the bottom reflector (cm)	121
Equivalent thickness of the side reflector (cm)	78
Density of the reflector graphite (g/cm <sup>3</sup> )	1.76
Impurity content of equivalent to natural boron in the graphite (ppm)	4.8
Thickness of the top carbon brick with natural boron (cm)	40
Thickness of the bottom carbon brick with natural boron (cm)	30
Thickness of the bottom carbon brick without natural boron (cm)	70
Equivalent thickness of the side carbon brick with natural boron (cm)	22
Density of the carbon brick (g/cm <sup>3</sup> )	1.59
Mass content of B <sub>4</sub> C in carbon brick with natural boron (%)	5
Radius of helium flow channels (cm)	4
Distance between the center of the helium channel and the centre of core (cm)	145
Radius of control rod channels and irradiation channels (cm)	6.5
Distance between the center of the control rod channel and the centre of core (cm)	102
<i>Boron absorber ball channels</i>	
Ellipsoid shape (cm)	16x6
Distance between the center of the channel and the centre of core (cm)	99

**Table 2.**

Physical Parameter	Unit	Value
<b>Fuel Element</b>		
Volumetric filling fraction of the fuel and the graphite balls in the core	%	61
Heavy metal uranium weight in each fuel element	g	5
Enrichment of <sup>235</sup> U (weight)	%	17
Diameter of fuel element	cm	6
Diameter of fuel zone in the fuel element	cm	5
Density of graphite in the matrix and outer shell of the fuel element	g/cm <sup>3</sup>	1.73
Impurity content of equivalent to natural boron in uranium	ppm	4
Impurity content of equivalent to natural boron in graphite	ppm	1.3
<b>Coated Particle</b>		
<b>Fuel Kernel</b>		
Radius of kernel	Cm	0.025
Density of UO <sub>2</sub>	g/cm <sup>3</sup>	10.4
<b>Coating Layers</b>		
Density of low density pyrolytic carbon	g/cm <sup>3</sup>	1.1
Thickness of low density pyrolytic carbon	cm	0.009
Density of inner high density pyrolytic carbon	g/cm <sup>3</sup>	1.9
Thickness of inner high density pyrolytic carbon	cm	0.004
Density of silicon carbide	g/cm <sup>3</sup>	3.18
Thickness of silicon carbide	cm	0.0035
Density of outer high density pyrolytic carbon	g/cm <sup>3</sup>	1.9
Thickness of outer high density pyrolytic carbon	cm	0.004
<b>Graphite Shell</b>		
Diameter of ball	cm	6
Density of graphite	g/cm <sup>3</sup>	1.84
Impurity content of equivalent to natural boron in graphite	ppm	0.125

**Table 3.**

Active Core Height (cm)	U-235 content in core (calculated-in g)	U-235 content in core (reference-in g)*	Relative mass Difference (g)	$k_{eff}$ (calculated)	$k_{eff}$ (reference)*	Absolute Relative Error in $k_{eff}$ (%)
150	9974.5	9974.8	-0.3	1.0822	1.0792	.2779
140	9310.2	9310.1	0.1	1.0592	1.0545	.4457
130	8646.0	8644.5	2.5	1.0338	1.0291	.4567
120	7981.7	7979.8	1.9	1.0055	.99888	.6627
110	7317.5	7315.1	2.4	.97371	.96443	.9622
100	6653.2	6649.6	3.6	.93764	.92530	1.333

\* HTR-10 results are taken as reference

**Table 4.**

Active Core Height (cm)	U-235 content in core (calculated-in g)	U-235 content in core (reference-in g)*	Relative mass Difference (g)	$k_{eff}$ (calculated)	$k_{eff}$ (reference)*	Absolute Relative Error in $k_{eff}$ (%)
150	9974.5	9974.8	-0.3	1.0793	1.0768	.2322
140	9310.2	9310.1	0.1	1.0565	1.0521	.4182
130	8646.0	8644.5	2.5	1.0312	1.0266	.4481
120	7981.7	7979.8	1.9	1.0028	.99634	.6484
110	7317.5	7315.1	2.4	.97108	.96305	.8338
100	6653.2	6649.6	3.6	.93502	.92266	1.339

\* HTR-10 results are taken as reference

**Table 5**

Physical Parameters	Unit	Value
Power	MW <sub>th</sub>	10
Core volume	m <sup>3</sup>	5.0
Core equivalent diameter	cm	180
Core equivalent height	cm	196.5
Number of fuel-graphite balls in the core		27 000
Inlet temperature of helium	°C	250
Outlet temperature of helium	°C	700
Mass flow rate of the helium in primary circuit	kg/s	4.32
Helium pressure in primary circuit	MPa	3.0
Average power density	W/ cm <sup>3</sup>	2.0
Average power generated in a single fuel element	kW	0.37
Peak power generated in a single fuel element	kW	0.55

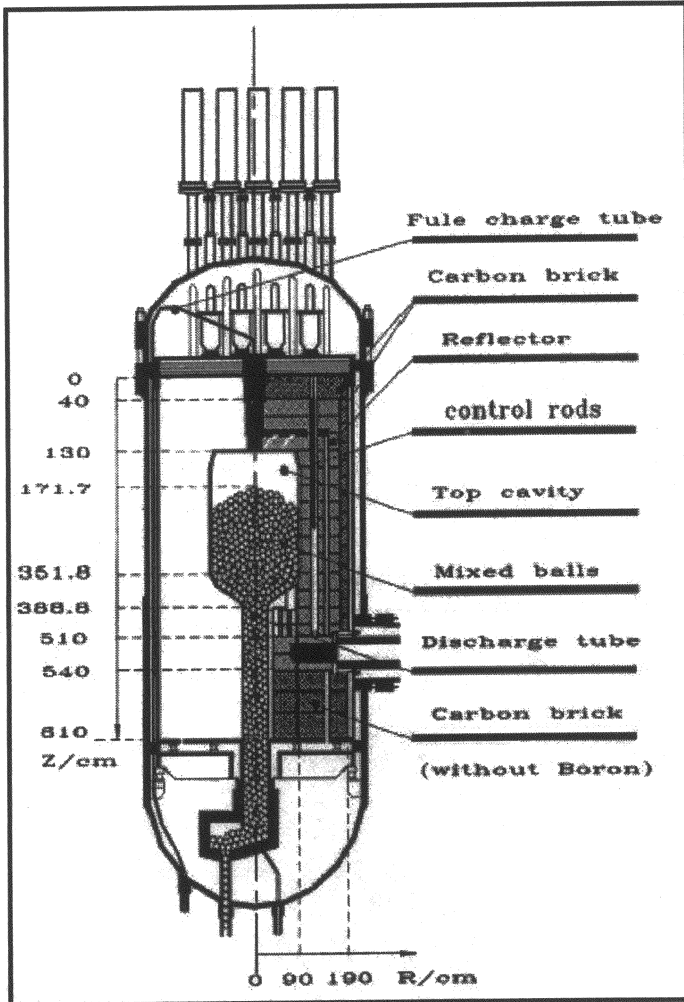


Figure 1.

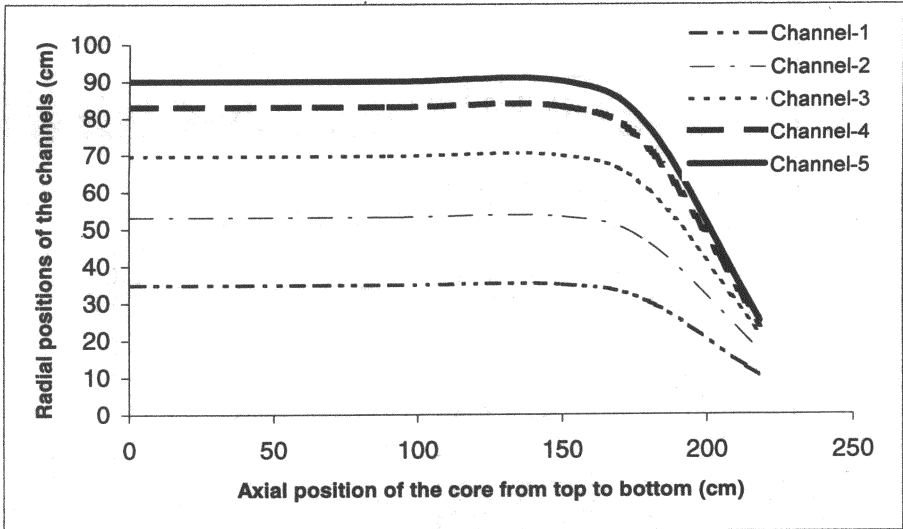


Figure 2.

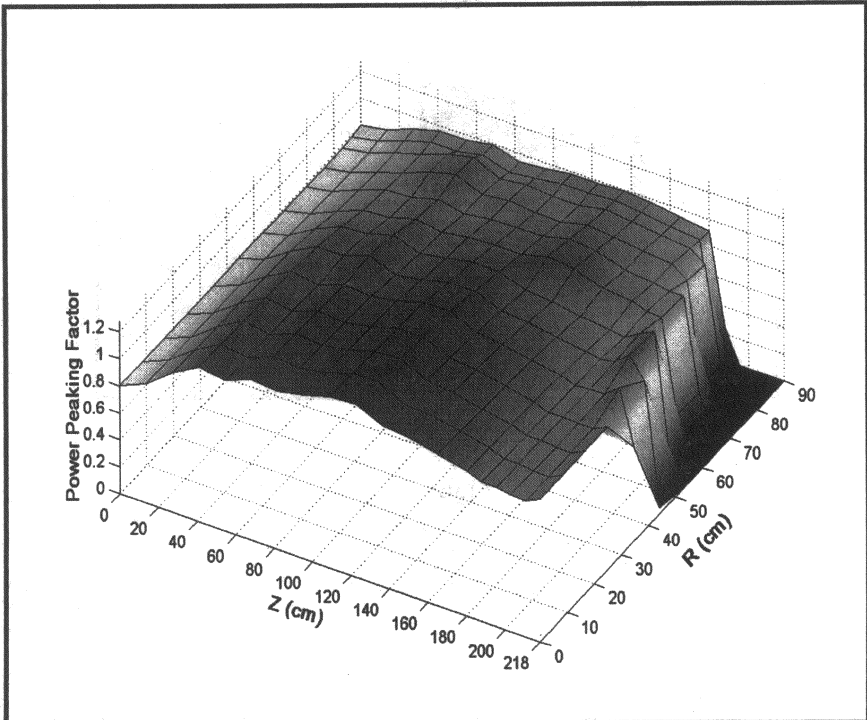


Figure 3.

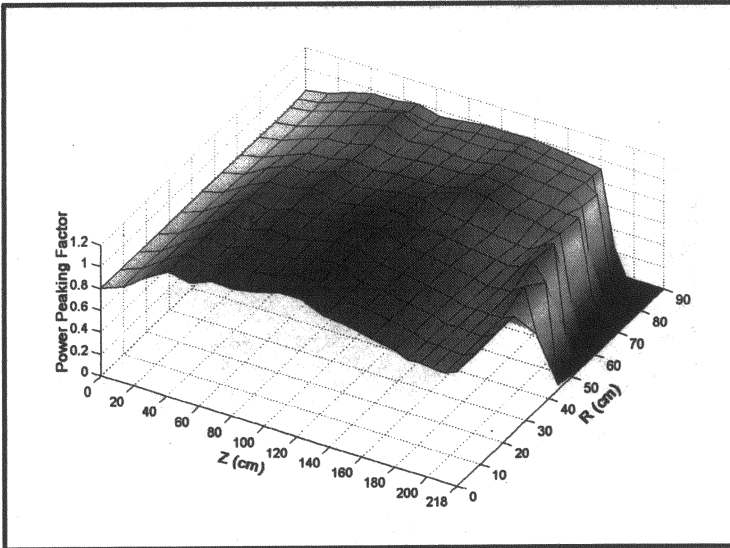


Figure 4.

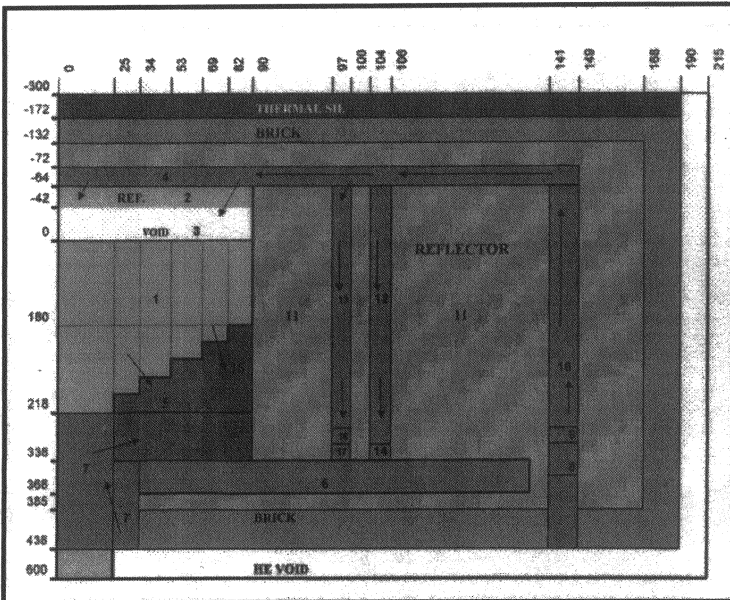


Figure 5.

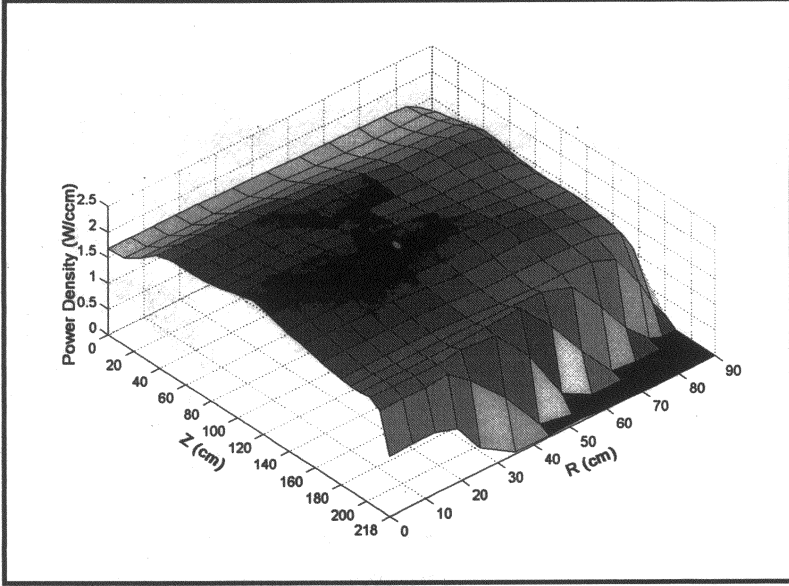


Figure 6.

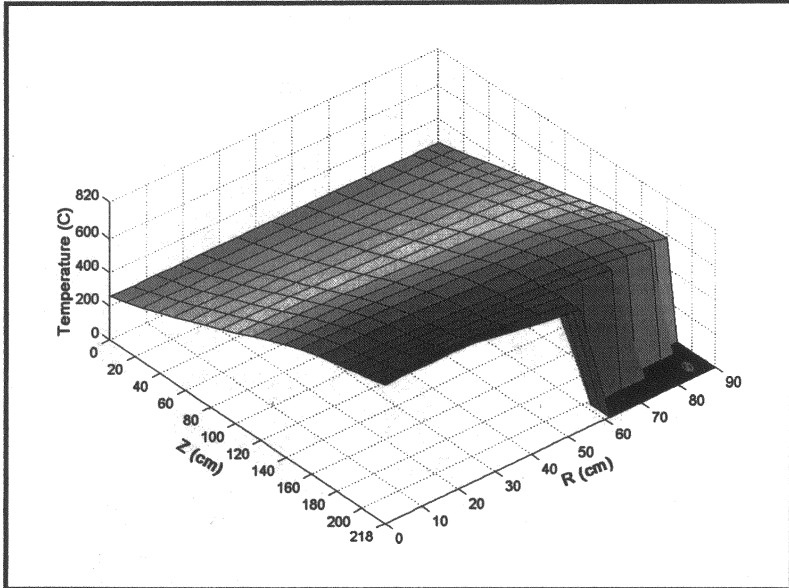


Figure 7.



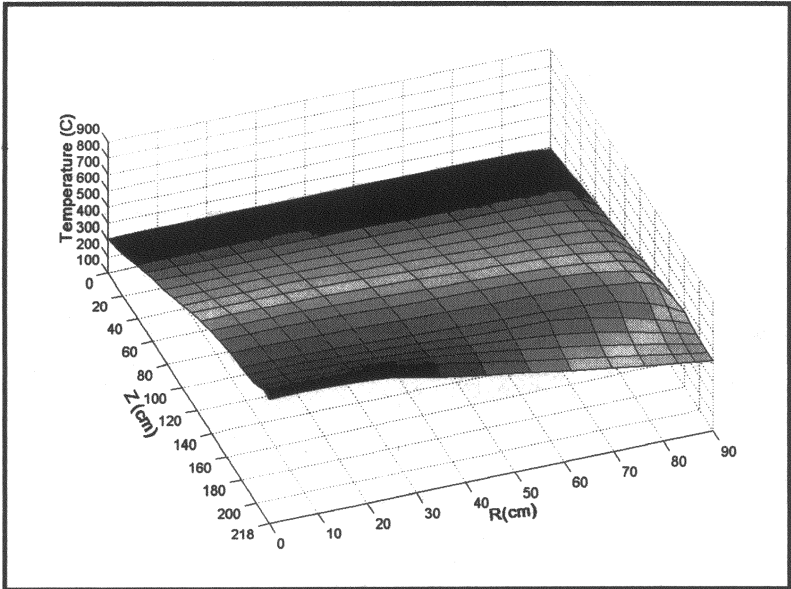


Figure 8.

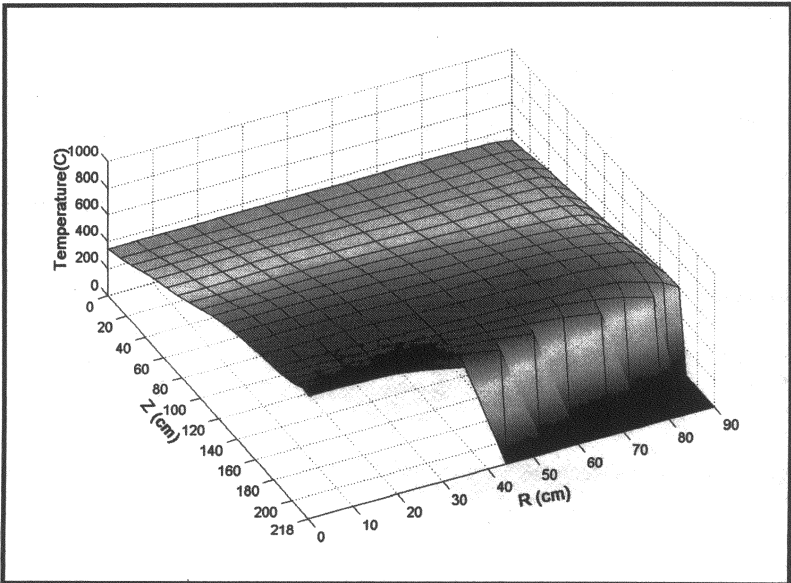


Figure 9.

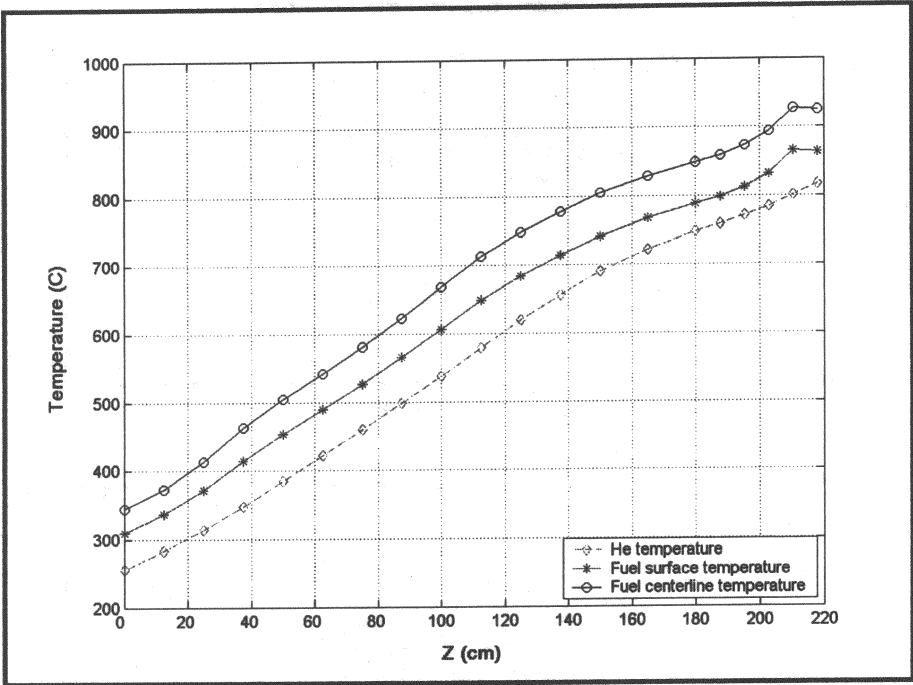


Figure 10.